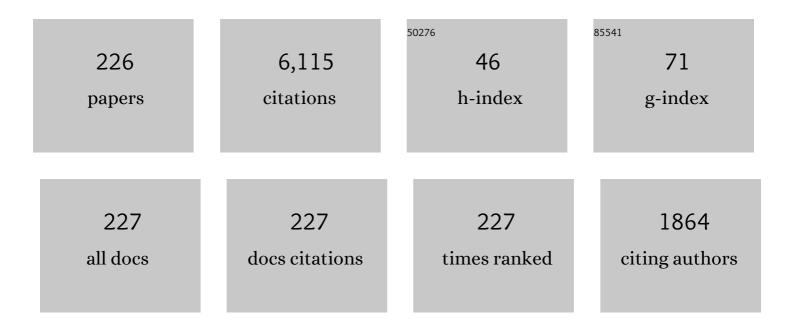
Vincenzo Spagnolo

List of Publications by Year in descending order

Source: https://exaly.com/author-pdf/4726062/publications.pdf Version: 2024-02-01



#	Article	IF	CITATIONS
1	Quartz-Enhanced Photoacoustic Spectroscopy: A Review. Sensors, 2014, 14, 6165-6206.	3.8	336
2	Photoacoustic Techniques for Trace Gas Sensing Based on Semiconductor Laser Sources. Sensors, 2009, 9, 9616-9628.	3.8	182
3	Recent advances in quartz enhanced photoacoustic sensing. Applied Physics Reviews, 2018, 5, .	11.3	174
4	Part-per-trillion level SF_6 detection using a quartz enhanced photoacoustic spectroscopy-based sensor with single-mode fiber-coupled quantum cascade laser excitation. Optics Letters, 2012, 37, 4461.	3.3	142
5	NO trace gas sensor based on quartz-enhanced photoacoustic spectroscopy and external cavity quantum cascade laser. Applied Physics B: Lasers and Optics, 2010, 100, 125-130.	2.2	131
6	Quartz enhanced photoacoustic H2S gas sensor based on a fiber-amplifier source and a custom tuning fork with large prong spacing. Applied Physics Letters, 2015, 107, .	3.3	128
7	Atmospheric CH4 measurement near a landfill using an ICL-based QEPAS sensor with V-T relaxation self-calibration. Sensors and Actuators B: Chemical, 2019, 297, 126753.	7.8	127
8	Measurement of subband electronic temperatures and population inversion in THz quantum-cascade lasers. Applied Physics Letters, 2005, 86, 111115.	3.3	123
9	Ppb-level detection of nitric oxide using an external cavity quantum cascade laser based QEPAS sensor. Optics Express, 2011, 19, 24037.	3.4	122
10	Intracavity quartz-enhanced photoacoustic sensor. Applied Physics Letters, 2014, 104, .	3.3	115
11	Analysis of the electro-elastic properties of custom quartz tuning forks for optoacoustic gas sensing. Sensors and Actuators B: Chemical, 2016, 227, 539-546.	7.8	110
12	Optical sensor for real-time monitoring of CO_2 laser welding process. Applied Optics, 2001, 40, 6019.	2.1	107
13	Terahertz quartz enhanced photo-acoustic sensor. Applied Physics Letters, 2013, 103, .	3.3	107
14	Widely-tunable mid-infrared fiber-coupled quartz-enhanced photoacoustic sensor for environmental monitoring. Optics Express, 2014, 22, 28222.	3.4	93
15	Ultra-high sensitive trace gas detection based on light-induced thermoelastic spectroscopy and a custom quartz tuning fork. Applied Physics Letters, 2020, 116, .	3.3	90
16	Single-tube on-beam quartz-enhanced photoacoustic spectroscopy. Optics Letters, 2016, 41, 978.	3.3	88
17	Quartz tuning forks resonance frequency matching for laser spectroscopy sensing. Photoacoustics, 2022, 25, 100329.	7.8	87
18	Quartz-enhanced photoacoustic spectroscopy for multi-gas detection: A review. Analytica Chimica Acta, 2022, 1202, 338894.	5.4	79

#	Article	IF	CITATIONS
19	A quartz enhanced photo-acoustic gas sensor based on a custom tuning fork and a terahertz quantum cascade laser. Analyst, The, 2014, 139, 2079-2087.	3.5	77
20	Tuning forks with optimized geometries for quartz-enhanced photoacoustic spectroscopy. Optics Express, 2019, 27, 1401.	3.4	77
21	THz Quartz-enhanced photoacoustic sensor for H_2S trace gas detection. Optics Express, 2015, 23, 7574.	3.4	76
22	Ppt level carbon monoxide detection based on light-induced thermoelastic spectroscopy exploring custom quartz tuning forks and a mid-infrared QCL. Optics Express, 2021, 29, 25100.	3.4	76
23	High and flat spectral responsivity of quartz tuning fork used as infrared photodetector in tunable diode laser spectroscopy. Applied Physics Reviews, 2021, 8, .	11.3	76
24	Thermal modeling of GalnAsâ^•AllnAs quantum cascade lasers. Journal of Applied Physics, 2006, 100, 043109.	2.5	73
25	Allan Deviation Plot as a Tool for Quartz-Enhanced Photoacoustic Sensors Noise Analysis. IEEE Transactions on Ultrasonics, Ferroelectrics, and Frequency Control, 2016, 63, 555-560.	3.0	72
26	Ultra-highly sensitive HCl-LITES sensor based on a low-frequency quartz tuning fork and a fiber-coupled multi-pass cell. Photoacoustics, 2022, 27, 100381.	7.8	72
27	Simultaneous measurement of the electronic and lattice temperatures in GaAs/Al0.45Ga0.55As quantum-cascade lasers: Influence on the optical performance. Applied Physics Letters, 2004, 84, 3690-3692.	3.3	70
28	Ppb-Level Quartz-Enhanced Photoacoustic Detection of Carbon Monoxide Exploiting a Surface Grooved Tuning Fork. Analytical Chemistry, 2019, 91, 5834-5840.	6.5	67
29	Mid-infrared fiber-coupled QCL-QEPAS sensor. Applied Physics B: Lasers and Optics, 2013, 112, 25-33.	2.2	66
30	Methane, ethane and propane detection using a compact quartz enhanced photoacoustic sensor and a single interband cascade laser. Sensors and Actuators B: Chemical, 2019, 282, 952-960.	7.8	66
31	Simultaneous dual-gas QEPAS detection based on a fundamental and overtone combined vibration of quartz tuning fork. Applied Physics Letters, 2017, 110, .	3.3	64
32	Atmospheric CH_4 and N_2O measurements near Greater Houston area landfills using a QCL-based QEPAS sensor system during DISCOVER-AQ 2013. Optics Letters, 2014, 39, 957.	3.3	62
33	Quartz-enhanced photoacoustic spectroscopy exploiting tuning fork overtone modes. Applied Physics Letters, 2015, 107, .	3.3	61
34	Terahertz quantum cascade lasers with large wall-plug efficiency. Applied Physics Letters, 2007, 90, 191115.	3.3	60
35	Improved Tuning Fork for Terahertz Quartz-Enhanced Photoacoustic Spectroscopy. Sensors, 2016, 16, 439.	3.8	59
36	In-plane quartz-enhanced photoacoustic spectroscopy. Applied Physics Letters, 2020, 116, .	3.3	59

#	Article	IF	CITATIONS
37	Temperature profile of GalnAs/AlInAs/InP quantum cascade-laser facets measured by microprobe photoluminescence. Applied Physics Letters, 2001, 78, 2095-2097.	3.3	58
38	Highly sensitive gas leak detector based on a quartz-enhanced photoacoustic SF6 sensor. Optics Express, 2016, 24, 15872.	3.4	57
39	Analysis of overtone flexural modes operation in quartz-enhanced photoacoustic spectroscopy. Optics Express, 2016, 24, A682.	3.4	57
40	Ppb-level gas detection using on-beam quartz-enhanced photoacoustic spectroscopy based on a 28ÂkHz tuning fork. Photoacoustics, 2022, 25, 100321.	7.8	57
41	Dual-Gas Quartz-Enhanced Photoacoustic Sensor for Simultaneous Detection of Methane/Nitrous Oxide and Water Vapor. Analytical Chemistry, 2019, 91, 12866-12873.	6.5	53
42	Temperature Dependence of Thermal Conductivity and Boundary Resistance in THz Quantum Cascade Lasers. IEEE Journal of Selected Topics in Quantum Electronics, 2008, 14, 431-435.	2.9	52
43	Multi-pass quartz-enhanced photoacoustic spectroscopy-based trace gas sensing. Optics Letters, 2021, 46, 977.	3.3	52
44	Light-induced thermo-elastic effect in quartz tuning forks exploited as a photodetector in gas absorption spectroscopy. Optics Express, 2020, 28, 19074.	3.4	51
45	Broadband detection of methane and nitrous oxide using a distributed-feedback quantum cascade laser array and quartz-enhanced photoacoustic sensing. Photoacoustics, 2020, 17, 100159.	7.8	47
46	Thermal properties of THz quantum cascade lasers based on different optical waveguide configurations. Applied Physics Letters, 2006, 89, 021111.	3.3	46
47	Overtone resonance enhanced single-tube on-beam quartz enhanced photoacoustic spectrophone. Applied Physics Letters, 2016, 109, .	3.3	46
48	Fiber-ring laser intracavity QEPAS gas sensor using a 7.2â€ [−] kHz quartz tuning fork. Sensors and Actuators B: Chemical, 2018, 268, 512-518.	7.8	46
49	Quartz-enhanced photoacoustic sensor for ethylene detection implementing optimized custom tuning fork-based spectrophone. Optics Express, 2019, 27, 4271.	3.4	46
50	Compact and portable quartz-enhanced photoacoustic spectroscopy sensor for carbon monoxide environmental monitoring in urban areas. Photoacoustics, 2022, 25, 100318.	7.8	45
51	Hydrogen peroxide detection with quartz-enhanced photoacoustic spectroscopy using a distributed-feedback quantum cascade laser. Applied Physics Letters, 2014, 104, .	3.3	44
52	Purely wavelength- and amplitude-modulated quartz-enhanced photoacoustic spectroscopy. Optics Express, 2016, 24, 25943.	3.4	44
53	Quartz–enhanced photoacoustic spectrophones exploiting custom tuning forks: a review. Advances in Physics: X, 2017, 2, 169-187.	4.1	44
54	Influence of InAs, AlAs δlayers on the optical, electronic, and thermal characteristics of strain-compensated GaInAsâ^•AlInAs quantum-cascade lasers. Applied Physics Letters, 2007, 91, .	3.3	43

#	Article	IF	CITATIONS
55	Quartz-enhanced photoacoustic spectroscopy for hydrocarbon trace gas detection and petroleum exploration. Fuel, 2020, 277, 118118.	6.4	43
56	Quartz-enhanced photoacoustic spectroscopy exploiting low-frequency tuning forks as a tool to measure the vibrational relaxation rate in gas species. Photoacoustics, 2021, 21, 100227.	7.8	43
57	Low-Loss Hollow Waveguide Fibers for Mid-Infrared Quantum Cascade Laser Sensing Applications. Sensors, 2013, 13, 1329-1340.	3.8	42
58	Partial Least-Squares Regression as a Tool to Retrieve Gas Concentrations in Mixtures Detected Using Quartz-Enhanced Photoacoustic Spectroscopy. Analytical Chemistry, 2020, 92, 11035-11043.	6.5	42
59	Mid-Infrared Quartz-Enhanced Photoacoustic Sensor for ppb-Level CO Detection in a SF ₆ Gas Matrix Exploiting a T-Grooved Quartz Tuning Fork. Analytical Chemistry, 2020, 92, 13922-13929.	6.5	42
60	High finesse optical cavity coupled with a quartz-enhanced photoacoustic spectroscopic sensor. Analyst, The, 2015, 140, 736-743.	3.5	41
61	High-concentration methane and ethane QEPAS detection employing partial least squares regression to filter out energy relaxation dependence on gas matrix composition. Photoacoustics, 2022, 26, 100349.	7.8	41
62	Electron-lattice coupling in bound-to-continuum THz quantum-cascade lasers. Applied Physics Letters, 2006, 88, 241109.	3.3	38
63	Thermal Modeling of Terahertz Quantum-Cascade Lasers: Comparison of Optical Waveguides. IEEE Journal of Quantum Electronics, 2008, 44, 680-685.	1.9	38
64	A quartz-enhanced photoacoustic sensor for H2S trace-gas detection at 2.6Âμ4m. Applied Physics B: Lasers and Optics, 2015, 119, 21-27.	2.2	37
65	H2S quartz-enhanced photoacoustic spectroscopy sensor employing a liquid-nitrogen-cooled THz quantum cascade laser operating in pulsed mode. Photoacoustics, 2021, 21, 100219.	7.8	37
66	Quantum Cascade Laser-Based Photoacoustic Sensor for Trace Detection of Formaldehyde Gas. Sensors, 2009, 9, 2697-2705.	3.8	36
67	Improved thermal management of mid-IR quantum cascade lasers. Journal of Applied Physics, 2008, 103, .	2.5	35
68	Nitrous oxide quartz-enhanced photoacoustic detection employing a broadband distributed-feedback quantum cascade laser array. Applied Physics Letters, 2018, 113, .	3.3	34
69	Parts-per-billion detection of carbon monoxide: A comparison between quartz-enhanced photoacoustic and photothermal spectroscopy. Photoacoustics, 2021, 22, 100244.	7.8	34
70	Thermal resistance and temperature characteristics of GaAs/Al0.33Ga0.67As quantum-cascade lasers. Applied Physics Letters, 2001, 78, 1177-1179.	3.3	33
71	Double antinode excited quartz-enhanced photoacoustic spectrophone. Applied Physics Letters, 2017, 110, .	3.3	33
72	Subband electronic temperatures and electron-lattice energy relaxation in terahertz quantum cascade lasers with different conduction band offsets. Applied Physics Letters, 2006, 89, 131114.	3.3	32

#	Article	IF	CITATIONS
73	Single mode operation with mid-IR hollow fibers in the range 51-105 µm. Optics Express, 2015, 23, 195.	3.4	32
74	Loss Mechanisms Determining the Quality Factors in Quartz Tuning Forks Vibrating at the Fundamental and First Overtone Modes. IEEE Transactions on Ultrasonics, Ferroelectrics, and Frequency Control, 2018, 65, 1951-1957.	3.0	29
75	Environmental Monitoring of Methane with Quartz-Enhanced Photoacoustic Spectroscopy Exploiting an Electronic Hygrometer to Compensate the H2O Influence on the Sensor Signal. Sensors, 2020, 20, 2935.	3.8	29
76	Time-resolved measurement of the local lattice temperature in terahertz quantum cascade lasers. Applied Physics Letters, 2008, 92, 101116.	3.3	28
77	Fiber-Coupled Quartz-Enhanced Photoacoustic Spectroscopy System for Methane and Ethane Monitoring in the Near-Infrared Spectral Range. Molecules, 2020, 25, 5607.	3.8	28
78	Raman scattering in CdTe1-xSex and CdS1-xSex nanocrystals embedded in glass. Superlattices and Microstructures, 1994, 16, 51-54.	3.1	27
79	Electronic distribution in superlattice quantum cascade lasers. Applied Physics Letters, 2000, 77, 1088-1090.	3.3	27
80	Coupling external cavity mid-IR quantum cascade lasers with low loss hollow metallic/dielectric waveguides. Applied Physics B: Lasers and Optics, 2012, 108, 255-260.	2.2	27
81	Sub-ppb-level CH ₄ detection by exploiting a low-noise differential photoacoustic resonator with a room-temperature interband cascade laser. Optics Express, 2020, 28, 19446.	3.4	27
82	Acoustic Coupling between Resonator Tubes in Quartz-Enhanced Photoacoustic Spectrophones Employing a Large Prong Spacing Tuning Fork. Sensors, 2019, 19, 4109.	3.8	26
83	Nonequilibrium optical phonon generation by steady-state electron transport in quantum-cascade lasers. Applied Physics Letters, 2002, 80, 4303-4305.	3.3	25
84	Nanoscale heat transfer in quantum cascade lasers. Physica E: Low-Dimensional Systems and Nanostructures, 2008, 40, 1780-1784.	2.7	25
85	Optical and Electronic NOx Sensors for Applications in Mechatronics. Sensors, 2009, 9, 3337-3356.	3.8	25
86	Quartz-enhanced photoacoustic NH3 sensor exploiting a large-prong-spacing quartz tuning fork and an optical fiber amplifier for biomedical applications. Photoacoustics, 2022, 26, 100363.	7.8	25
87	Experimental investigation of the lattice and electronic temperatures in Ga0.47In0.53Asâ^•Al0.62Ga0.38As1â^'xSbx quantum-cascade lasers. Applied Physics Letters, 2007, 90, 121109.	3.3	24
88	Modulation cancellation method for measurements of small temperature differences in a gas. Optics Letters, 2011, 36, 460.	3.3	23
89	Modulation cancellation method for isotope ^180/^160 ratio measurements in water. Optics Express, 2012, 20, 3401.	3.4	23
90	Thermal characteristics of quantum-cascade lasers by micro-probe optical spectroscopy. IEE Proceedings: Optoelectronics, 2003, 150, 298.	0.8	22

#	Article	IF	CITATIONS
91	Low-Loss Coupling of Quantum Cascade Lasers into Hollow-Core Waveguides with Single-Mode Output in the 3.7–7.6 μm Spectral Range. Sensors, 2016, 16, 533.	3.8	21
92	Modulation cancellation method in laser spectroscopy. Applied Physics B: Lasers and Optics, 2011, 103, 735-742.	2.2	20
93	Hollow core waveguide as mid-infrared laser modal beam filter. Journal of Applied Physics, 2015, 118, 113102.	2.5	20
94	Octupole electrode pattern for tuning forks vibrating at the first overtone mode in quartz-enhanced photoacoustic spectroscopy. Optics Letters, 2018, 43, 1854.	3.3	20
95	Compact quartz-enhanced photoacoustic sensor for ppb-level ambient NO2 detection by use of a high-power laser diode and a grooved tuning fork. Photoacoustics, 2022, 25, 100325.	7.8	20
96	Photoacoustic spectroscopy for gas sensing: A comparison between piezoelectric and interferometric readout in custom quartz tuning forks. Photoacoustics, 2020, 17, 100155.	7.8	19
97	Detection of ultrafast laser ablation using quantum cascade laser-based sensing. Applied Physics Letters, 2012, 101, .	3.3	18
98	Influence of the band-offset on the electronic temperature of GaAs/Al(Ga)As superlattice quantum cascade lasers. Semiconductor Science and Technology, 2004, 19, S110-S112.	2.0	17
99	Front-End Amplifiers for Tuning Forks in Quartz Enhanced PhotoAcoustic Spectroscopy. Applied Sciences (Switzerland), 2020, 10, 2947.	2.5	16
100	Mid-infrared intracavity quartz-enhanced photoacoustic spectroscopy with pptv – Level sensitivity using a T-shaped custom tuning fork. Photoacoustics, 2022, 25, 100330.	7.8	16
101	Experimental determination of the temperature distribution in trench-confined oxide vertical-cavity surface-emitting lasers. IEEE Journal of Quantum Electronics, 2003, 39, 701-707.	1.9	15
102	Thermoelastic stress in GaAs/AlGaAs quantum cascade lasers. Applied Physics Letters, 2003, 82, 4639-4641.	3.3	15
103	Phonons in Si/GaAs superlattices. Physical Review B, 1992, 46, 7296-7299.	3.2	13
104	Damping Mechanisms of Piezoelectric Quartz Tuning Forks Employed in Photoacoustic Spectroscopy for Trace Gas Sensing. Physica Status Solidi (A) Applications and Materials Science, 2019, 216, 1800552.	1.8	13
105	Si-GaAs(001) superlattice structure. Journal of Crystal Growth, 1993, 127, 121-125.	1.5	12
106	Piezo-enhanced acoustic detection module for mid-infrared trace gas sensing using a grooved quartz tuning fork. Optics Express, 2019, 27, 35267.	3.4	12
107	Mid infrared quantum cascade laser operating in pure amplitude modulation for background-free trace gas spectroscopy. Optics Express, 2016, 24, 26464.	3.4	11
108	Phytoextraction from Chromium-Contaminated Soil Using Moso Bamboo in Mediterranean Conditions. Water, Air, and Soil Pollution, 2020, 231, 1.	2.4	11

#	Article	IF	CITATIONS
109	Quartz-Enhanced Photoacoustic Detection of Ethane in the Near-IR Exploiting a Highly Performant Spectrophone. Applied Sciences (Switzerland), 2020, 10, 2447.	2.5	11
110	Siâ€GaAs(001) superlattices. Applied Physics Letters, 1992, 61, 1570-1572.	3.3	10
111	Phytoextraction of Cr(VI)-Contaminated Soil by Phyllostachys pubescens: A Case Study. Toxics, 2021, 9, 312.	3.7	10
112	Sensitive detection of nitric oxide using a 5.26 μm external cavity quantum cascade laser based QEPAS sensor. Proceedings of SPIE, 2012, , .	0.8	9
113	Simultaneous multi-gas detection between 3 and 4 μm based on a 2.5-m multipass cell and a tunable Fabry-Pérot filter detector. Spectrochimica Acta - Part A: Molecular and Biomolecular Spectroscopy, 2019, 216, 154-160.	3.9	9
114	Hot-phonon generation in THz quantum cascade lasers. Journal of Physics: Conference Series, 2007, 92, 012018.	0.4	8
115	Spatial mode filtering of mid-infrared (mid-IR) laser beams with hollow core fiber optics. Proceedings of SPIE, 2013, , .	0.8	8
116	Electronic temperatures of terahertz quantum cascade active regions with phonon scattering assisted injection and extraction scheme. Optics Express, 2013, 21, 10172.	3.4	8
117	Hot Electrons in THz Quantum Cascade Lasers. Journal of Infrared, Millimeter, and Terahertz Waves, 2013, 34, 357-373.	2.2	7
118	Mode matching of a laser-beam to a compact high finesse bow-tie optical cavity for quartz enhanced photoacoustic gas sensing. Sensors and Actuators A: Physical, 2017, 267, 70-75.	4.1	7
119	Compact and Versatile QEPAS-Based Sensor Box for Simultaneous Detection of Methane and Infrared Absorber Gas Molecules in Ambient Air. Frontiers in Environmental Chemistry, 0, 3, .	1.6	7
120	Excitons and electron-phonon interaction in In0.52Ga0.18Al0.30As layers. Solid State Communications, 1992, 84, 679-683.	1.9	6
121	Fröhlich electron-phonon interaction in CdSxSe1-xnanocrystals. Superlattices and Microstructures, 1995, 18, 113-120.	3.1	6
122	On Line Sensing of Ultrafast Laser Microdrilling Processes by Optical Feedback Interferometry. Physics Procedia, 2013, 41, 670-676.	1.2	6
123	Influence of Air Pressure on the Resonance Properties of a T-Shaped Quartz Tuning Fork Coupled with Resonator Tubes. Applied Sciences (Switzerland), 2021, 11, 7974.	2.5	6
124	Application of standard and custom quartz tuning forks for quartz-enhanced photoacoustic spectroscopy gas sensing. Applied Spectroscopy Reviews, 2023, 58, 562-584.	6.7	6
125	<title>Optical sensor for real-time weld defect detection</title> ., 2002, , .		5
126	Trace gas sensing using quantum cascade lasers and a fiber-coupled optoacoustic sensor: Application to formaldehyde. Journal of Physics: Conference Series, 2010, 214, 012037.	0.4	5

#	Article	IF	CITATIONS
127	Quantum-cascade-laser-based optoacoustic detection for breath sensor applications. , 2011, , .		5
128	Facet temperature mapping of GaAs/AlGaAs quantum cascade lasers by photoluminescence microprobe. Optical Materials, 2001, 17, 219-222.	3.6	4
129	Direct measurement of the local temperature distribution in oxide VCSELs. , 2002, , .		4
130	Quartz-enhanced photoacoustic spectroscopy for gas sensing applications. , 2020, , 597-659.		4
131	Evidence of electronic confinement in pseudomorphic Si/GaAs superlattices. Physical Review B, 1998, 57, R15100-R15103.	3.2	3
132	<title>Nondestructive technique for the direct measurement of the local temperature distribution in VCSELs</title> . , 2002, 4648, 22.		3
133	Non equilibrium electrons in THz quantum cascade lasers. , 2006, 6133, 126.		3
134	Mid-IR quantum cascade laser mode coupling in hollow-core, fiber-optic waveguides with single-mode beam delivery. Proceedings of SPIE, 2015, , .	0.8	3
135	Influence of Tuning Fork Resonance Properties on Quartz-Enhanced Photoacoustic Spectroscopy Performance. Sensors, 2019, 19, 3825.	3.8	3
136	Modeling and Design of a Semi-Integrated QEPAS Sensor. Journal of Lightwave Technology, 2021, 39, 646-653.	4.6	3
137	Partial least squares regression as novel tool for gas mixtures analysis in quartz-enhanced photoacoustic spectroscopy. , 2020, , .		3
138	Vibrational properties of Si/GaAs superlattices. Superlattices and Microstructures, 1992, 12, 429-432.	3.1	2
139	Hot electron effects and nanoscale heat transfer in Terahertz quantum cascade lasers. Proceedings of SPIE, 2009, , .	0.8	2
140	Mid-infrared quantum cascade laser based trace gas technologies: Recent progress and applications in health and environmental monitoring. , 2011, , .		2
141	THz quartz-enhanced photoacoustic sensor employing a quantum cascade laser source. Proceedings of SPIE, 2013, , .	0.8	2
142	New approaches in quartz-enhanced photoacoustic sensing. Proceedings of SPIE, 2015, , .	0.8	2
143	Innovative quartz enhanced photoacoustic sensors for trace gas detection. , 2016, , .		2
144	New Developments in Quartz-Enhanced Photoacoustic Sensing Real-World Applications. , 2020, , .		2

New Developments in Quartz-Enhanced Photoacoustic Sensing Real-World Applications. , 2020, , . 144

#	Article	IF	CITATIONS
145	Quantum Cascade Laser Technology for the Ultrasensitive Detection of Low-Level Nitric Oxide. Methods in Molecular Biology, 2011, 704, 115-133.	0.9	2
146	Compact and low-noise quartz-enhanced photoacoustic sensor for sub-ppm ethylene detection in atmosphere. , 2018, , .		2
147	Recent advances in quartz-enhanced photoacoustic sensing. , 2018, , .		2
148	One- and two-phonon scattering processes in ZnSe/ZnSxSe1â^'xsuperlattices studied by micro-Raman spectroscopy. Physical Review B, 1994, 50, 4988-4991.	3.2	1
149	Quantum-well-laser mirror degradation investigated by microprobe optical spectroscopy. , 1995, , .		1
150	2-D temperature mapping of vertical-cavity surface-emitting lasers determined by microprobe electroluminescence. IEEE Photonics Technology Letters, 2002, 14, 266-268.	2.5	1
151	Electronic spatial distribution of In0.53Ga0.47Asâ^•AlAs0.56Sb0.44 quantum-cascade lasers. Journal of Applied Physics, 2005, 98, 086106.	2.5	1
152	Electronic and lattice temperatures in bound-to-continuum terahertz quantum cascade lasers. , 2006, , .		1
153	Electronic and thermal properties of Sb-based QCLs operating in the first atmospheric window. , 2007, , \cdot		1
154	Microprobe photoluminescence assessment of the wall-plug efficiency in interband cascade lasers. Journal of Applied Physics, 2008, 104, 046101.	2.5	1
155	Photoacoustic trace gas sensing with mid-IR quantum cascade lasers. , 2009, , .		1
156	Modulation cancellation method (MOCAM) in modulation spectroscopy. , 2011, , .		1
157	Sensitive Detection of Nitric Oxide Using a Quantum Cascade Laser Based QEPAS Sensor. , 2012, , .		1
158	Cavity and quartz enhanced photo-acoustic mid-IR sensor. , 2013, , .		1
159	THz quantum cascade laser-based quartz enhanced photo-acoustic sensor. , 2013, , .		1
160	Quartz-enhanced photoacoustic sensors for H2S trace gas detection. , 2015, , .		1
161	New developments in THz quartz enhanced photoacoustic spectroscopy. , 2016, , .		1
162	Modeling the dependence of fork geometry on the performance of quartz enhanced photoacoustic		1

spectroscopic sensors., 2015,,.

#	Article	IF	CITATIONS
163	Interband cascade laser based quartz-enhanced photoacoustic sensor for multiple hydrocarbons detection. , 2018, , .		1
164	Simultaneous dual gas QEPAS sensing of water and methane/nitrous oxide. , 2019, , .		1
165	Simultaneous measurement of N2O, CH4, and NH3 with a compact quartz-enhanced photoacoustic sensor for monitoring agricultural activities. , 2022, , .		1
166	Measurement of the methane isotopologues relaxation rate exploiting quartz-enhanced photoacoustic spectroscopy. , 2022, , .		1
167	Well width dependence of electron-phonon interaction in ZnSe/ZnSxSe1-x superlattices determined by micro-raman spectroscopy. Superlattices and Microstructures, 1994, 16, 47-49.	3.1	0
168	<title>Peak optical power and thermal performance of quantum cascade lasers</title> ., 2001, , .		0
169	State of the art of InP and GaAs quantum cascade lasers. , 0, , .		0
170	Simultaneous measurement of the electronic and lattice temperatures in GaAs quantum cascade lasers and their correlation with the optical performance. , 0, , .		0
171	Electronic and Thermal properties of THz Quantum Cascade. , 2006, , .		0
172	Experimental measurement of the wall-plug efficiency in THz quantum cascade lasers. , 2007, , .		0
173	High performance THz quantum cascade laser with different optical waveguide configurations. , 2007, , .		0
174	Correlation between the subband electronic temperatures and the internal quantum efficiency of THz quantum cascade lasers. , 2008, , .		0
175	Time of flight measurements of the nanoscale heat transfer dynamic in terahertz quantum cascade lasers. , 2009, , .		0
176	Trace gas sensing using quantum cascade lasers and optoacoustic detection. Proceedings of SPIE, 2009, , .	0.8	0
177	Quantum-cascade-laser-based optoacoustic detection: application to nitric oxide and formaldehyde. Proceedings of SPIE, 2010, , .	0.8	0
178	Advanced optoacoustic sensor designs for environmental applications. Proceedings of SPIE, 2010, , .	0.8	0
179	Mid-infrared quantum cascade laser based trace gas sensor technologies: Recent advances and applications. , 2011, , .		0

180 Modulation cancellation method for laser spectroscopy. , 2011, , .

0

#	Article	IF	CITATIONS
181	Spectroscopic measurements of isotopic water composition using a new modulation cancellation method. , 2012, , .		0
182	Electronic temperature in phonon-photon-phonon terahertz quantum cascade devices with high-operating temperature performance. , 2013, , .		0
183	Part-per-trillion level detection of SF ₆ using a single-mode fiber-coupled quantum cascade laser and a quartz enhanced photoacoustic sensor. Proceedings of SPIE, 2013, , .	0.8	0
184	Quantum cascade laser-based sensing to investigate fast laser ablation process. , 2013, , .		0
185	Quantum cascade laser-based sensor system for hydrogen peroxide detection. , 2013, , .		0
186	Measurement of relative velocity of independent targets by a quantum cascade laser subject to optical feedback. , 2014, , .		0
187	New spectrophone designs based on a quartz tuning fork. , 2016, , .		0
188	Recent advances of the quartz-enhanced photoacoustic trace gas detection technique. , 2016, , .		0
189	Hollow-core waveguide for single-mode laser beam propagation in the spectral range of 3.7-7.3 l̂¼m. , 2016, , .		0
190	Quartz enhanced photoacoustic leak sensor for mechatronic components. Proceedings of SPIE, 2016, ,	0.8	0
191	Quartz tuning forks with novel geometries for optoacoustic gas sensing. , 2016, , .		0
192	Pure amplitude and wavelength modulation spectroscopy for detection of N2O using a three-section quantum cascade laser. , 2017, , .		0
193	Low power consumption quartz-enhanced photoacoustic gas sensor employing a quantum cascade laser in pulsed operation. Proceedings of SPIE, 2017, , .	0.8	0
194	Single-tube on beam quartz-enhanced photoacoustic spectrophones exploiting a custom quartz tuning fork operating in the overtone mode. Proceedings of SPIE, 2017, , .	0.8	0
195	Recent advances in quartz-enhanced photoacoustic sensors employing custom tuning fork operating at the first overtone flexural mode. , 2017, , .		0
196	Broadband Gas QEPAS Detection Exploiting a Monolithic DFB-QCL Array. NATO Science for Peace and Security Series B: Physics and Biophysics, 2021, , 61-70.	0.3	0
197	Quartz-enhanced photoacoustic spectroscopy of methane isotopologues. , 2021, , .		0
198	Quartz-enhanced photoacoustic spectroscopy for CO detection in SF6 decomposition. , 2021, , .		0

#	Article	IF	CITATIONS
199	Quartz tuning forks employed as photodetectors in TDLAS sensors. , 2021, , .		0
200	Experimental Investigation of Hot Carriers in Terahertz Quantum Cascade Lasers. Acta Physica Polonica A, 2008, 113, 787-794.	0.5	0
201	Modulation-cancellation method for laser spectroscopy. SPIE Newsroom, 0, , .	0.1	0
202	Modulation cancellation method for spectroscopic measurements. , 2012, , .		0
203	Quartz Enhanced Photoacoustic Sensors for Trace Gas Detection in the IR and THz Spectral Range. NATO Science for Peace and Security Series B: Physics and Biophysics, 2014, , 139-151.	0.3	0
204	Recent advances of mid–infrared compact, field deployable sensors and their real world applications in the petrochemical industry, atmospheric chemistry and security. , 2016, , .		0
205	Micro-resonator Parameter Optimization of a QEPAS Spectrophone using a Custom Quartz Tuning Fork with large Prong Spacing. , 2016, , .		0
206	Recent advances and applications of mid-infrared semiconductor based trace gas sensor technologies. , 2016, , .		0
207	Recent advances in quartz enhanced photoacoustic sensing. , 2017, , .		0
208	Trace gas spectroscopy using state-of-the- art mid-infrared semiconductor laser sources: progress, status, and applications. , 2017, , .		0
209	Tapered hollow-core fibers providing single-mode output in the 3.5um-7.8um spectral range. , 2018, , .		0
210	High Performance Mid-IR Devices and Applications to Gas Sensing. , 2018, , .		0
211	Fiber Laser Intracavity Quartz-Enhanced Photoacoustic Gas Sensor. , 2018, , .		0
212	New Developments in Quartz-Enhanced Photoacoustic Spectroscopy for Gas Sensing Applications. , 2018, , .		0
213	New generation of tuning forks for quartz-enhanced photoacoustic spectroscopy. , 2019, , .		0
214	Quartz-enhanced photoacoustic sensors for detection of multiple hydrocarbon and methane isotopes. , 2019, , .		0
215	Octupole electrode pattern for tuning forks vibrating at the first overtone mode in quartz-enhanced photoacoustic spectroscopy. , 2019, , .		0
216	Quartz-enhanced photoacoustic spectroscopy employing a distributed feedback-quantum cascade laser array for nitrous oxide and methane broadband detection. , 2019, , .		0

#	Article	IF	CITATIONS
217	Measurement of non-radiative gas molecules relaxation rates by using quartz-enhanced photoacoustic spectroscopy. , 2020, , .		0
218	Intracavity quartz-enhanced photoacoustic spectroscopy for CO/N2O detection in the part-per-trillion concentration range. , 2020, , .		0
219	Fiber-coupled quartz-enhanced photoacoustic sensor for methane and ethane trace detection. , 2020, ,		0
220	N2-cooled THz quartz-enhanced photoacoustic sensor operating in pulsed mode for hydrogen sulfide detection in the part-per-billion concentration range. , 2020, , .		0
221	Comparison between interferometric and piezoelectric readout of tuning fork vibrations in quartz-enhanced photoacoustic spectroscopy. , 2020, , .		0
222	A novel double-tuning fork acoustic detection module for photoacoustic wide range sensing. , 2022, ,		0
223	Compact sensor for wide concentration range methane and ethane detection employing quartz tuning fork as photodetector in tunable diode laser spectroscopy. , 2022, , .		0
224	Quartz enhanced photoacoustic spectrometer for natural gas composition analysis. , 2022, , .		0
225	Quartz-enhanced photoacoustic spectroscopy employing a Vernier-effect distributed feedback-quantum cascade laser for multiple analytes detection. , 2022, , .		0
226	Quartz-enhanced photoacoustic sensors for environmental monitoring applications. , 2022, , .		0